Unified Performance Theory for V/STOL Aircraft in Equilibrium Flight. Part II

T. STRAND,* E. S. LEVINSKY,† AND M. H. Y. WEI‡
Air Vehicle Corporation, La Jolla, Calif.

This is the second of a two-part paper dealing with the minimum power requirements of V/STOL aircraft. A unified performance theory was developed in Part I. In Part II, the cross-sectional area associated with apparent mass concepts is calculated for several different ducted and unshrouded wing-propeller combinations.

A. Minimum Induced Drag of Duct and Wing Combinations

MINIMUM induced drag for a given lift is obtained when the "downwash velocity" is constant throughout a perpendicular section of the wake at infinity downstream.[1] This constant downwash w_∞ is defined as the induced velocity normal to the longitudinal direction of the essentially rectilinear vortex wake emanating from the trailing edge of the wing-duct combination.

The total kinetic energy T of all the fluid particles in each unit strip in the longitudinal direction of the wake is, from classical finite wing theory,

$$T = (\rho/2)\Sigma_\infty w_\infty^2 \tag{1}$$

where by definition

$$\Sigma_\infty = 4\int_0^{b/2}\left(\frac{\Phi}{w_\infty}\right)dy - A_s \tag{2}$$

Here, Φ is the velocity potential in the Trefftz plane (w_∞ being the velocity at infinity), and A_s denotes the sum of the cross-sectional areas of the slip streams. It is implicitly assumed that the airplane configuration exhibits symmetry about both the vertical and horizontal axes.

The kinetic energy per unit time can then be expressed as follows:

$$D_{i\infty}V_\infty = TV_\infty\cos\epsilon = \tfrac{1}{2}(\rho\Sigma_\infty V_\infty\cos\epsilon)w_\infty^2 \tag{3}$$

The term in brackets is usually termed the apparent or virtual mass. Σ_∞ is therefore a cross-sectional area associated with apparent mass.

Classical finite wing theory assumes the downwash angle ϵ to be small, i.e., $\cos\epsilon \simeq 1$. In this case, the normal force is essentially equal to the airplane lift L_∞. In the absence of slip stream effects ($V_\infty = V_s$), we find $L_\infty = (\rho\Sigma_\infty V_\infty)w_\infty$ by momentum considerations. By eliminating w_∞, we arrive at the following basic equation of classical wing theory:

$$D_{i\infty} = L_\infty^2/2\rho V_\infty^2\Sigma_\infty \tag{4}$$

Then, defining nondimensional coefficients, and noting that for the special case of a monoplane wing the cross-sectional area $\Sigma_\infty = \pi b^2/4$, we find the well known relation $C_{Di}/C_L^2 = 1/\pi AR$.

It is apparent from the previous discussion that the main task of calculating lift and drag in the optimum case reduces to the problem of finding potential solutions to the Laplace equation in the Trefftz plane for given configurations. In the following section, the potential solutions for various twin duct and wing combinations will be determined. As far as is known, these solutions have not previously appeared in the technical literature.

A1. Two Ducts with Interconnecting Wing plus Wing Tips

Consider the V/STOL configuration depicted in Fig. 1. Because the slip streams behind the ducts neither contract nor expand, the dimensions of the wake far downstream are identical to those of the airplane under consideration. For the optimum case, the wing and twin-duct wakes move downward like a solid body.

The basic idea is now to map this contour, the flow velocity potential of which we do not know, into another simpler contour the velocity potential of which is already known. The contour of the wake is first mapped into an indented rectangle (see Fig. 1) by the complex-variable transformation:

$$S = (i/2\pi)\ln[(Z + y_0)/(Z - y_0)] \tag{5}$$

where $Z = y + iz$. The constant y_0 may be determined by the theorem of Apollonius and is found to be

$$y_0 = \{[(b/2) - R - P]^2 - R^2\}^{1/2} \tag{6}$$

where P is the length of the wing tip outside the slip stream.

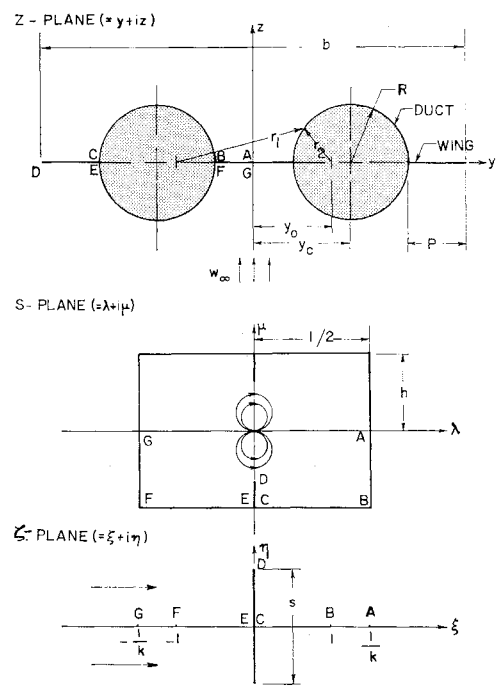

Fig. 1 Conformal mapping planes for two ducts with interconnecting wing plus wing tips.

Received February 12, 1966; revision received November 23, 1966. Part I of this paper was published in the March-April 1967 issue of the *Journal of Aircraft*. [3.01]

* President. Associate Fellow AIAA.

† Vice President. Member AIAA.

‡ Staff Scientist.

The region exterior to the wake contour in the physical Z plane is thereby mapped conformally into the interior of the rectangle in the S plane. It may also be recognized that the flow from infinity in the Z plane is now transformed into a flow from a doublet located at the origin of the S plane.

Because the indented rectangle is still not a sufficiently good contour, we must employ one more transformation, namely

$$S = \frac{1}{2K}\int_0^{\zeta} \frac{dt}{(1-t^2)(1-k^2t^2)} - ih \tag{7}$$

where $K(k)$ = the complete elliptic integral of the first kind with modulus $k(0 \leq k \leq 1)$. Through this equation, the

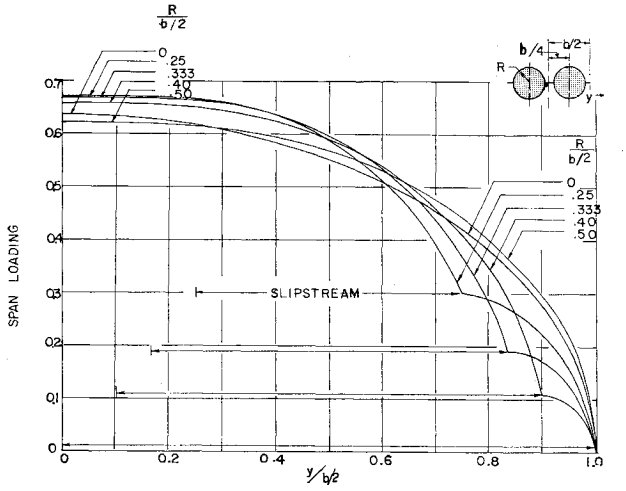

Fig. 2 Trefftz-plane span loadings for minimum induced drag of twin duct and wing combinations.

lower half of the inside of the indented rectangle is transformed into the entire upper half of the ζ plane. The doublet at the origin of the S plane reverts to a uniform flow from infinity in the ζ plane. The boundary of the original contour is now represented by the ξ axis and part of the η axis, as shown in Fig. 1.

The velocity potential for this flow is finally recognizable as a flow past a flat plate of total width s mounted at right angle to the stream, namely

$$F = \Phi + i\psi = (2/\pi)w_\infty y_0 k K[\zeta^2 + (s/2)^2]^{1/2} \tag{8}$$

The constant in front of the term in large brackets has been determined by satisfying the condition that the velocity in the physical plane at infinity shall be w_∞. For complete problem determination, we have two constants yet to be calculated, namely k and s.

The half height of the indented rectangle is determined by the airplane geometry ratios as follows:

$$h = \frac{1}{2\pi}\ln \frac{\left[1-\frac{2R}{b/2}-\frac{P}{b/2}\right]+\left[\left(1-\frac{R}{b/2}-\frac{P}{b/2}\right)^2-\left(\frac{R}{b/2}\right)^2\right]^{1/2}}{\left[1-\frac{2R}{b/2}-\frac{P}{b/2}\right]-\left[\left(1-\frac{R}{b/2}-\frac{P}{b/2}\right)^2-\left(\frac{R}{b/2}\right)^2\right]^{1/2}} \tag{9}$$

Once h is calculated for a given configuration, the modulus k of the transformation (7) is determined by mapping point $A(\frac{1}{2}, 0)$ of the S plane into the arbitrary point $A(1/k, 0)$ in the ζ plane. This yields the following relation for determination of k:

$$K(k')/2K(k) = h \tag{10}$$

The length of the wing tip segment $\overline{CD}$ in the S plane is found to be

$$\overline{CD} = h - \frac{1}{2\pi}\ln\left[\frac{1+y_0/(b/2)}{1-y_0/(b/2)}\right] \tag{11}$$

and the total width s of the flat plate in the ζ plane is determined from the same length through the following relation:

$$\overline{CD} = F[k', \tan^{-1}(s/2)]/2K(k) \tag{12}$$

where $F[k', \tan^{-1}(s/2)]$ = the incomplete elliptic integral of the first kind with modulus $k' = (1-k^2)^{1/2}$ and amplitude $\tan^{-1}(s/2)$.

After determination of s, the velocity potential in the Z plane is known. By Eq. (2), Σ_∞ may therefore now be calculated.

In Fig. 3 of Part I (previous issue) are presented results of numerical calculations for the special case when the ducts are mounted at the center of the half spans. It is noted that the values of Σ_∞ are quite close to $\pi b^2/4$ over most of the range. The corresponding span loadings of the solid wake at infinity downstream, which, by the way, are not indicative of the actual span loadings of the airplane, are shown in Fig. 2. These loadings in the Trefftz plane would be needed by anyone wanting to determine the actual span loadings using strip theory. The Trefftz-plane span loadings have been calculated in the conventional manner from the following formula:

$$\frac{l}{L} = \frac{\Phi}{2\int_0^{b/2}\Phi dy} \tag{13}$$

A2. Two Ducts with Interconnecting Wing

In this section, we shall consider the same configuration as was analyzed in the previous section, with, however, the wing tips removed (Fig. 1). The contour is thereby simplified. With very few modifications, the equations of Sec. A1 may be used to obtain the new velocity potential.

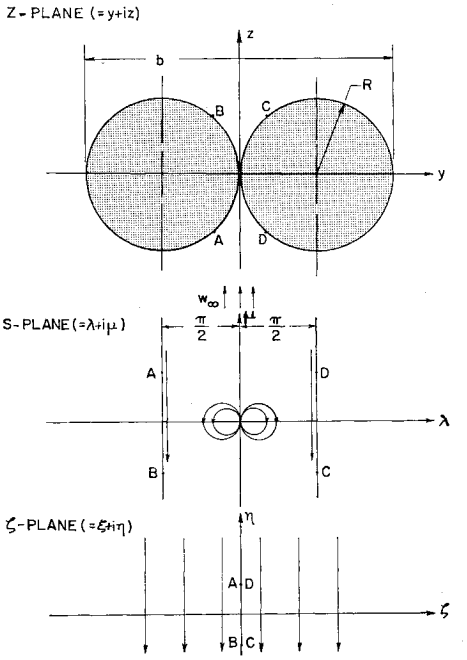

Fig. 3 Conformal mapping planes for two touching ducts.

By applying the transformation (5), we once more map the contour of the physical Z plane into a rectangle in the S plane. This time, however, the rectangle is not indented. Then, the boundary of the rectangle in the S plane is transformed into the ξ axis of the ζ plane through use of Eq. (7). The corresponding complex potential in the ζ plane is now simply that of a uniform flowfield, namely

$$F = \Phi + i\psi = (2/\pi)w_\infty y_0 k K\zeta \tag{14}$$

We observe that the potential in this case depends only upon the single parameter k, which is a function of the geometry ratio $R/(b/2)$. To calculate k, we first set $P/(b/2)$ equal to zero in Eq. (9). The value of h is, therefore, again known when $R/(b/2)$ is given. By use of Eq. (10), the value of k is readily calculated. Finally, the value of y_0 is obtained from Eq. (6).

The results of the numerical calculations for this particular configuration are shown graphically in Fig. 3 of Part I (previous issue). It is seen that the curve lies above the one obtained in the previous section.

A3. Two Touching Ducts

When the span of the interconnecting wing is reduced to zero, the transformation (5) becomes singular and is no longer valid. A different transformation is required in this case. It was decided to map the exterior of the physical contour into an infinite strip between two parallel plates (see Fig. 3) through the relation

$$S = \pi b/4Z \tag{15}$$

The uniform flow from infinity in the Z plane is thereby transformed into a flow from a doublet located at the origin of the S plane. The problem is then to find a velocity potential yielding zero normal velocity on the plate. Applying the additional mapping,

$$\zeta = \cot S \tag{16}$$

the doublet at the origin in the S plane is transformed into a uniform flow from infinity in the ζ plane. The two plates in the S plane are mapped into the entire η axis of the ζ plane. The complex potential in this plane may then be expressed as follows:

$$F = \Phi + i\psi = -iw_\infty(\pi b/4)\zeta \tag{17}$$

In the physical plane, the velocity potential becomes

$$\Phi = -Re\{iw_\infty(\pi b/4)\cot[\pi b/4(y + iz)]\} \tag{18}$$

On the surface of the two neighboring cylinders, this reduces to

$$\Phi/w_\infty = (\pi b/4)\tanh(\pi z/2y) \tag{19}$$

Combining Eqs. (2) and (19), the size of the cross-sectional area associated with apparent mass is found to be

$$\Sigma_\infty = 1.163\pi b^2/4 \qquad \text{for} \qquad R/(b/2) = \tfrac{1}{2} \tag{20}$$

This value yields the proper end point for the two curves determined in Sec. A1 and A2 (Fig. 3 of Part I, previous issue).

A4. Four Ducts

The calculation of cross-sectional areas associated with apparent mass for V/STOL configurations having four ducts mounted side by side and touching each other, or four ducts with interconnecting wings, has not been attempted here. Instead, we obtain an estimate of Σ_∞ by recognizing this configuration as being somewhat similar to a rectangle of the same span with height equal to one duct diameter. The flow around a rectangle is given in Durand.[2] We have here removed from the tabulated Durand values the contribution

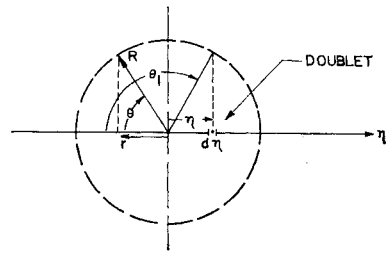

Fig. 4 Coordinates for single unshrouded propeller and wing combination.

to Σ_∞ from the flow inside (or through) the rectangle by subtracting the inside area [see Eq. (2)]. The result is presented graphically in Fig. of Part I (previous issue), and shows a remarkable similar trend to the case of two ducts with an interconnecting wing. The values given for a rectangle might well be used for engineering purposes in the absence of more accurate data.

B. Minimum Induced Drag of Wing and Unshrouded Propeller Combinations

The boundary conditions across the outer edge of the slip stream are

$$\Phi_s V_s = \Phi_\infty V_\infty \quad \text{and} \quad V_\infty(\partial\Phi_s/\partial n) = V_s(\partial\Phi_\infty/\partial n) \tag{21}$$

where Φ_s and Φ_∞ are the velocity potentials inside and outside the slip stream, respectively, and V_s and V_∞ are the corresponding axial velocities. Glauert[3] used these boundary conditions, together with the "method of images" for reflecting the elementary wing vortices in the slip-stream boundary, to solve the problem of a wing in an open jet wind tunnel (equivalent to a wing in a slip stream at zero forward speed). The analysis to be presented here is partly an extension of Glauert's work to arbitrary forward speeds.

Squire and Chester[4] have calculated the span loading for minimum induced drag by expanding the potential inside and outside the slip stream into two separate series, which satisfy Eqs. (21) term by term. The coefficients in the series are evaluated by matching with the far field solution. Their method, although applicable for multipropeller wing combinations, converges very slowly when the slip stream boundary is close to the wing tip and when V_∞ is small compared to V_s. On the other hand, the image method is difficult to carry out for more than the single propeller and wing combination, except at zero forward speed.

In the present treatment, use is made of both methods. The method of images is used to obtain the apparent mass for single propeller configurations at all V_∞ and for multipropeller configurations at $V_\infty = 0$. The series expansion procedure is used for multipropeller configurations at large forward speeds. The apparent mass is then interpolated over the intervening low forward speed regime.

The present analysis for minimum induced drag is carried out in the Trefftz plane, in which effects of the bound vortex disappear. Other analyses[5,6] using lifting surface and slender body theories apply to the direct calculation of wing lift.

B1. Single Propeller with Wing Spanning the Slip Stream

The vortex wake of a wing-propeller combination can be visualized as formed by a series of infinitesimal horseshoe vortices, or by doublets of strength $\Gamma d\eta$, where $\Gamma(\eta)$ is the circulation distribution across the span (Fig. 4). For a single propeller of diameter $2R = b$, the vortex wake is entirely within the slip stream, and the optimum condition for the downwash velocity $w_s(r)$ becomes simply[5]

$$\frac{w_s}{V_s} = -\frac{1}{4\pi V_s}\int_{-R}^{R}\frac{(d\Gamma/d\eta)d\eta}{(\eta - r)} + \frac{\lambda_s R^2}{4\pi V_s r}\int_{-R}^{R}\frac{(d\Gamma/d\eta)}{(\eta r - R^2)}\,d\eta = \text{const} \tag{22}$$

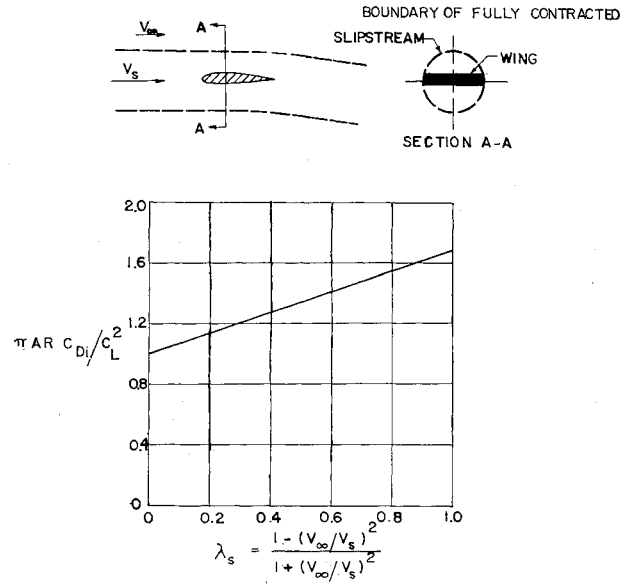

Fig. 5 Minimum induced drag with power. Single unshrouded propeller with planar wing spanning the slip stream. (Coefficients based upon slip-stream dynamic pressure.)

The solution of this integral equation for $\Gamma(\eta)$ was obtained by Glauert for the case of a rectangular wing in an open jet tunnel ($\lambda_s = 1$) at a given angle of attack. Here we will adapt Glauert's procedure for solving Eq. (22) to the minimum induced drag problem over the entire velocity range $0 \leq \lambda_s \leq 1$.

Setting $r = -R\cos\theta$ and $\eta = -R\cos\theta_1$ (see Fig. 4), and writing

$$\Gamma(\eta) = 4RV_s \sum_{n=1,3,5\ldots} A_n \sin n\theta_1$$

where the A_n are unknown coefficients, Eq. (22) becomes

$$\frac{w_s}{V_s} = \frac{1}{\pi}\int_0^\pi \sum_{n=1,3,5,\ldots} nA_n \left\{ \frac{\cos n\theta_1}{(\cos\theta_1 - \cos\theta)} + \frac{\lambda_s}{\cos\theta}\cdot\frac{\cos n\theta_1}{(1 - \cos\theta_1\cos\theta)} \right\} d\theta_1 \quad (23)$$

The θ_1 integration may be carried out directly giving

$$\frac{w_s}{V_s} = \sum_n \frac{nA_n}{\sin\theta}\left[\sin n\theta + \frac{\lambda_s(1-\sin\theta)^n}{(\cos\theta)^{n+1}}\right] \quad (24)$$

Following Glauert, we set

$$\frac{(1-\sin\theta)^n}{(\cos\theta)^{n+1}} = \sum_n rQ_{nr}\sin r\theta \quad (25)$$

where rQ_{nr} is the rth Fourier coefficient in the Fourier sine series expansion of $(1-\sin\theta)^n/(\cos\theta)^{n+1}$ over the interval $0 \leq \theta \leq \pi$. Thus

$$rQ_{nr} = \frac{2}{\pi}\int_0^\pi \frac{(1-\sin\theta)^n}{(\cos\theta)^{n+1}}\sin r\theta d\theta \quad (26)$$

Values of Q_{nr} are tabulated by Glauert for $n, r \leq 7$. In terms of the Q_{nr}, the downwash angle, Eq. (22), becomes

$$\frac{w_s}{V_s} = \sum_{n=1,3,\ldots}\frac{nA_n}{\sin\theta}\left[\sin n\theta + \lambda_s \sum_{r=1,3,\ldots} rQ_{nr}\sin r\theta\right] \quad (27)$$

This may now be readily solved for the A_n by multiplying by $(\sin m\theta \sin\theta)$ and integrating from $0 \leq \theta \leq \pi$. Recognizing that w_s/V_s = const (minimum induced drag) gives in

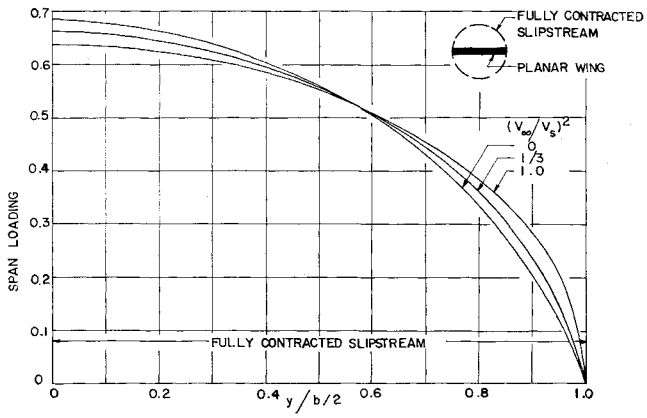

Fig. 6 Span loadings for minimum induced drag. Single unshrouded propeller and planar wing combination.

matrix form

$$-\lambda_s \begin{Bmatrix} Q_{31} \\ Q_{51} \\ \ldots \\ Q_{j1} \end{Bmatrix} = \begin{bmatrix} (1+3\lambda_s Q_{33}) & 5\lambda_s Q_{53}\ldots & j\lambda_s Q_{j3} \\ 3\lambda_s Q_{35} & (1+5\lambda_s Q_{55})\ldots & j\lambda_s Q_{j5} \\ \ldots & \ldots & \ldots \\ j\lambda_s Q_{3j} & j\lambda_s Q_{5j}\ldots & (1+j\lambda_s Q_{jj}) \end{bmatrix} \begin{Bmatrix} A_3/A_1 \\ A_5/A_1 \\ \ldots \\ A_j/A_1 \end{Bmatrix} \quad (28)$$

where j is the upper limit on n and r. Equation (28) was solved for $j = 7$ and $\lambda_s = 1, 0.75, 0.50, 0.25$, and 0. The resulting values of A_n/A_1 are listed in Table 1.

The total lift L and induced drag D_i are readily evaluated in terms of the A_n. As is well known, the lift is a function only of A_1, i.e.,

$$C_L = \pi(AR)A_1$$

The induced drag, on the other hand, is a function of all the A_n, and introducing the induced drag coefficient $C_{Di} = D_i/\frac{1}{2}\rho V_s^2 S$, we obtain

$$\frac{C_{Di}}{C_L^2} = \frac{1}{\pi AR}\left\{\sum_n n\left(\frac{A_n}{A_1}\right)^2 + \lambda_s \sum_m\sum_n mn\left(\frac{A_m}{A_1}\right)\left(\frac{A_n}{A_1}\right)Q_{nm}\right\} \quad (29)$$

In terms of the cross-sectional areas Σ_∞ and Σ_s associated with the outside and inside apparent masses, respectively, we may also write [see Eq. (28), Part I, previous issue]

$$C_{Di}/C_L^2 = (1/\pi AR)[(p^2\Sigma_\infty + \Sigma_s)/\pi b^2/4]^{-1} \quad (30)$$

The minimum induced drag coefficient and the term $(p^2\Sigma_\infty + \Sigma_s)$ may therefore be calculated for all ratios of V_∞/V_s by use of Eqs. (29) and (30) and Table 1. The results are presented in Fig. 5 and show that the ratio C_{Di}/C_L^2 increases apparently linearly with increasing λ_s. An increase in C_{Di}/C_L^2 with decreasing forward speed was, of course, to be

Table 1 A_n/A_1

	n			
λ_s	1	3	5	7
1.00	1	−0.09277	−0.03124	−0.01501
0.75	1	−0.07386	−0.02580	−0.01269
0.50	1	−0.05255	−0.01904	−0.00959
0.25	1	−0.02821	−0.01062	−0.00546
0	1	0	0	0

expected, since these coefficients are based upon the slip-stream dynamic pressure. As the speed decreases, a progressively smaller amount of mass would be involved in the momentum transfer in the Trefftz plane. The maximum of the minimum induced drag, namely $C_{Di}/C_L^2 = 1.68/\pi AR$, is then reached at zero forward speed. The corresponding cross-sectional area associated with apparent mass $\Sigma_s = (0.6)\pi b^2/4$ at $V_\infty = 0$.

The optimum span loadings of the configuration were determined in the usual manner. They are shown in Fig. 6. They are not elliptical, except of course at $V_\infty = V_s$. This may also be demonstrated by, for instance, calculating C_{Di}/C_L^2 for an elliptical span loading at zero forward speed and comparing with the optimum value. For the elliptic case, $A_1 = 1$ and $A_3 = A_5 = A_7 = 0$, and Eq. (29) yields $C_{Di}/C_L^2 = (1 + Q_{11})/\pi AR = 1.73/\pi AR$ for $V_\infty = 0$. This value is slightly higher than the minimum stated previously.

The corresponding values of the apparent mass area ($p^2\Sigma_\infty + \Sigma_s$) are shown in Fig. 6a of Part I (previous issue). It is also of interest to determine Σ_∞ and Σ_s separately as a function of forward velocity, since these are required in the unified V/STOL performance theory presented in Part I. At hover, we have already shown that $\Sigma_s = 0.6\pi b^2/4$. At the opposite endpoint of the velocity scale, the flow is reduced to the classical case of a flat plate moving downward with a constant velocity in a fluid of constant total head. Let us then determine Σ_s for this case. By classical finite wing theory, the kinetic energy may be written as follows:

$$T = -\frac{\rho}{2} \oint \varphi \frac{\partial \varphi}{\partial n}\, ds \tag{31}$$

where n and s denote, respectively, the inward normal and the tangent to the boundary of the region external to the vortex wake. The complex potential function is now given by

$$F = \varphi + i\psi = -iw_\infty[Z^2 - (b/2)^2]^{1/2} + iw_\infty Z$$

We may now use the previous expression in Eq. (31) and perform the line integration along the circular slip-stream boundary. It is then first necessary to determine φ, $\partial\varphi/\partial n$ and ds.

To separate φ from the complex function F, we introduce elliptical coordinates, i.e.,

$$y = (b/2)\cosh\mu\cos\lambda \qquad z = (b/2)\sinh\mu\sin\lambda$$

On the circle of radius $b/2$, $y^2 + z^2 = (b/2)^2$, and we find $\sinh\mu = \sin\lambda$. Substitution into the complex potential function, yields the velocity potential on the boundary of what previously was the slip stream, as follows:

$$\varphi_b = w_\infty(b/2)[(1 + \sin^2\lambda)^{1/2} - \sin\lambda]\sin\lambda \tag{32}$$

The complex velocity in the elliptical coordinates is given by

$$\frac{dF}{dz} = u - iv = w_\infty\left[-\left(\frac{\sin\lambda\cos\lambda}{\cosh^2\mu - \cos^2\lambda}\right) + i\left(1 - \frac{\sinh\mu\cosh\mu}{\cosh^2\mu - \cos^2\lambda}\right)\right] \tag{33}$$

At the boundary of the slip stream we, therefore, have

$$u = -(w_\infty/2)\cot\lambda \qquad v = w_\infty\left\{1 - \frac{(1 + \sin^2\lambda)^{1/2}}{2\sin\lambda}\right\}$$

Thus, with $\partial\varphi/\partial n = d\varphi/dr = u\cos\theta + v\sin\theta$, $\sin\theta = z/(b/2) = \sin^2\lambda$, and $\cos\theta = y/(b/2) = (1 + \sin^2\lambda)^{1/2}\cos\lambda$ on the boundary, it is easily seen that

$$\frac{\partial\varphi_b}{\partial n} = \frac{w_\infty}{2\sin\lambda}[2(1 + \sin^2\lambda)^{1/2}\sin^2\lambda - 2\sin^3\lambda - (1 + \sin^2\lambda)^{1/2}]$$

The expression for ds in elliptical coordinates can be found in a similar manner by writing $(ds)^2 = (dy)^2 + (dz)^2$, where

$$dy = (b/2)[\cos\lambda\sinh\mu d\mu - \cosh\mu\sin\lambda\, d\lambda]$$

$$dz = (b/2)[\sin\lambda\cosh\mu d\mu + \sinh\mu\cos\lambda d\lambda]$$

On the boundary $d\mu = (\cos\lambda/\cosh\mu)d\lambda$. Thus

$$ds = b[\sin\lambda/(1 + \sin^2\lambda)^{1/2}]d\lambda$$

Gathering up the previous information, the expression for the total kinetic energy outside the slip stream in a unit strip becomes

$$T = \frac{\rho}{2}\Sigma_\infty w_\infty^2 = -\frac{\rho}{2} w_\infty^2 b^2 \times \int_0^\pi \left[\frac{\sin^2\lambda}{(1 + \sin^2\lambda)^{1/2}} - \sin\lambda\right][2(1 + \sin^2\lambda)^{1/2}\sin^2\lambda - 2\sin^3\lambda - (1 + \sin^2\lambda)^{1/2}]d\lambda \tag{34}$$

Solving for Σ_∞ and performing the integration, give

$$\frac{\Sigma_\infty}{\pi b^2/4} = 1 - \frac{2}{\pi} = 0.363 \tag{35}$$

The value of $\Sigma_s/(\pi b^2/4)$ inside the slip stream is then $(1 - 0.363)$ or 0.637. We have now determined the value of $\Sigma_s/(\pi b^2/4)$ at either endpoint of the velocity range, namely 0.637 at $p = 1$ and 0.6 at $p = 0$. For intermediate values of p, a straight line interpolation is suggested until further data become available. The results so far obtained for a wing spanning a single slip stream are shown graphically in Fig. 6a of Part I (previous issue).

B2. Two Unshrouded Propellers and Wing at Cruise and Upper Transition Speed

If we assume that the deflection of the fully contracted slip stream due to propeller inclination is negligible at cruise and upper transition speeds, the wing-propeller theory of Squire and Chester[4] may be employed to obtain optimum span loadings and cross-sectional areas associated with apparent mass. This wing theory is restricted by series convergence difficulties to the region in which the velocity ratio V_∞/V_s is in the neighborhood of unity, i.e., to cruise and upper transition speeds. It is also applicable only when the tips of the monoplane wing penetrate some distance through the outboard slip streams. However, by extrapolation, it is possible to determine the cross-sectional areas of more conventional configurations in which the wing ends at the boundary of the outboard slip stream.

Squire and Chester calculated optimum span distributions for monoplane wings with single and twin slip streams. In this section, we shall extend their calculations to obtain the cross-sectional areas associated with apparent mass for the flow inside and outside the slip streams, separately. A condensed version of their twin propeller approach is given below to enable the reader to follow the development of the next section in which the Squire and Chester method is extended to cover the case of a wing with four propellers.

Let us now consider a monoplane wing submerged in a uniform stream of infinite extent with velocity V_∞. At infinity upstream, there are two side by side circular slip streams of velocity V_s. The freestream and the slip streams are parallel initially. The centers of the slip streams are located in the plane of the wing. The flowfields are analyzed in the Trefftz plane. Although it is realized that the boundaries of the two slip streams are no longer circular in this plane, it is assumed that they have undergone only a slight deformation, and that the conditions given by Eqs. (21) may be satisfied on the circles. The coordinate system used

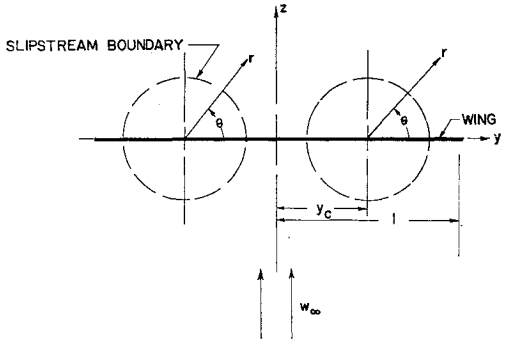

Fig. 7 Coordinate system for wing with two propellers.

is shown in Fig. 7. The wing half span will be taken to be unity. The optimizing condition of constant downwash angle is assumed, and the downward flow of the vortex wake in the Trefftz plane is stopped by superimposing a uniform upward velocity of magnitude w_∞.

Squire and Chester choose to employ the following velocity potentials which satisfy the given boundary conditions [Eqs. (21)] exactly and give zero downwash velocity along the vortex wake:

$$\Phi_\infty = w_\infty F \tag{36}$$

$$\Phi_s = w_\infty pf \tag{37}$$

where

$$F = a_0 + \sum_1^\infty a_n \left[\frac{1+p^2}{2}\left(\frac{r}{R}\right)^n + \frac{1-p^2}{2}\left(\frac{R}{r}\right)^n\right]\cos n\theta \tag{38}$$

$$= a_0 + \sum_1^\infty a_n \left(\frac{r}{R}\right)^n \cos n\theta \tag{39}$$

These potentials are, of course, harmonic functions. It should be noted that Φ_∞ yields an infinite velocity as $r \to \infty$. Thus, Φ_∞ is valid only in the immediate neighborhood of each circular boundary. The boundary conditions in the plane of the wing outside the wing tips and at infinity are not satisfied.

If we now view the Trefftz plane from far away, it is clear that the small slit, representing the vortex wake, and its two slip streams appear to be a line obstacle to the upward flow plus some type of doublet singularities located at the center of the slip streams. Therefore, the complex potential function $H(= \Phi + i\psi)$ at large $Z(= y + iz)$ may be written

$$H = (1 - Z^2)^{1/2}\left[1 - \frac{A_1}{Z^2 - y_c^2} - \frac{A_2}{(Z^2 - y_c^2)^2} \cdots\right] \tag{40}$$

The first term on the right-hand side is the potential function of a flow from infinity past a flat plate, and the fractions inside the large brackets represent the singularities, the first of which is recognized as being a doublet.

The harmonic functions F and f can also be represented by the real parts of the following complex functions:

$$H = a_0 + \sum_1^\infty a_n \left[\frac{1+p^2}{2}\left(\frac{Z_1}{R}\right)^n + \frac{1-p^2}{2}\left(\frac{R}{Z_1}\right)^n\right] \tag{41}$$

$$h = a_0 + \sum_1^\infty a_n \left(\frac{Z_1}{R}\right)^n \tag{42}$$

where by definition $Z_1 = Z - y_c$.

If we now expand Eq. (40) for small values of Z_1, Eqs. (40) and (41) should be identical, and unique relations between the A_n and the a_n can be established. Then, by the boundary conditions and Eq. (42), the unknown constants A_n can be determined. The expressions for these constants in the series expansion are somewhat lengthy and will be omitted here. Once the constants are found, the span loading is obtained in the conventional manner, i.e., the circulation strength $\Gamma_\infty(y) = 2\Phi_\infty$ and $\Gamma_s(y) = 2\Phi_s$, where the local lift $l = \rho V_\infty \Gamma_\infty$ at station y outside the slip stream and $l = \rho V_s \Gamma_s$ at station y inside the slip stream. The total lift L is then given by

$$L = \rho V_\infty^2 \epsilon \int_{\text{span outside slip stream}} (2\Phi_\infty)dy + \rho V_s^2 \epsilon \int_{\text{span inside slip stream}} (2\Phi_s)dy \tag{43}$$

The normalized lift distribution is simply l/L, and is found plotted in Fig. 8 for one selected value of $R/(b/2)$. The cross-sectional area Σ_s is obtained through another integration, i.e., from Eq. (31),

$$\Sigma_s = (-2/w_s^2) \oint_{\text{around upper (or lower) half of slip stream}} \Phi_s \times (\partial\Phi_s/\partial n)ds \tag{44}$$

By now writing the total lift

$$L = \rho V_\infty^2 \epsilon \Sigma_\infty + \rho V_s^2 \epsilon \Sigma_s \tag{45}$$

we can solve for Σ_∞, since L and Σ_s are known from Eqs. (43) and (44). The two cross-sectional areas Σ_∞ and Σ_s are found plotted in the summary graph, Fig. 6b of Part I (previous issue).

B3. Four Unshrouded Propellers and Wing at Cruise and Upper Transition Speeds

To extend Squire and Chester's method to the case of a monoplane wing with four propellers, we now assume that the complex potential function at large values of Z behaves as follows:

$$H = (1 - Z^2)^{1/2}\left[1 - \frac{A_1}{Z^2 - y_{c1}^2} - \frac{A_1'}{Z^2 - y_{c2}^2} - \frac{A_2}{(Z^2 - y_{c1}^2)^2} - \frac{A_2'}{(Z^2 - y_{c2}^2)^2} \cdots\right] \tag{46}$$

Defining two new variables, namely $Z_1 = Z - y_{c1}$ and $Z_2 = Z - y_{c2}$ with the origins located in the centers of the slip streams, the outside complex potential functions around, respectively, Z_1 and Z_2 may be written

$$H = a_0 + \sum_1^\infty a_n \left[\frac{1+p}{2}\left(\frac{Z_1}{R}\right)^n + \frac{1-p}{2}\left(\frac{R}{Z_1}\right)^n\right] \tag{47}$$

$$H' = a_0' + \sum_1^\infty a_n' \left[\frac{1+p}{2}\left(\frac{Z_2}{R}\right)^n + \frac{1-p}{2}\left(\frac{R}{Z_2}\right)^n\right] \tag{48}$$

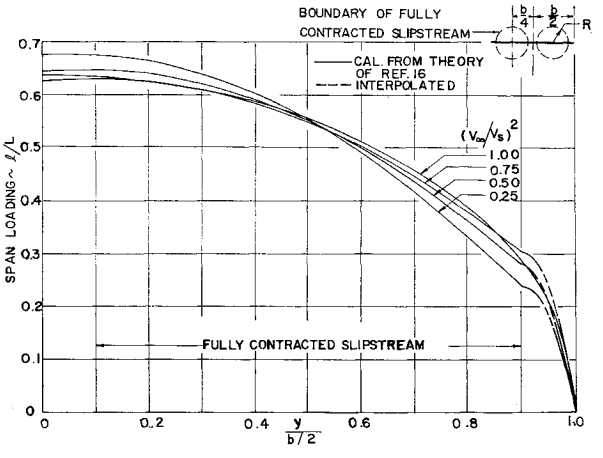

Fig. 8 Span loadings for minimum induced drag for two unshrouded propellers and wing combination at cruise and upper transition speeds, $R/(b/2) = 0.4$.

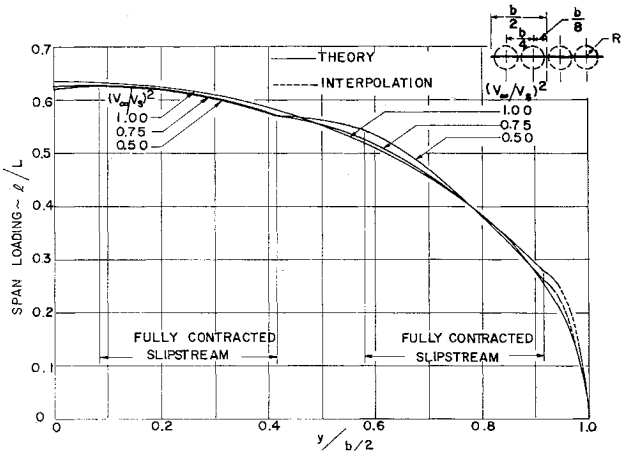

Fig. 9 Span loadings for minimum induced drag for four unshrouded propellers and wing combination at cruise and upper transition speeds, $R/(b/2) = \frac{1}{6}$.

By expanding Eq. (46) about Z_1 and Z_2 separately, we can determine the constants A_n as functions of a_n and a_n'. To satisfy the boundary conditions [Eqs. (21)], we use the following velocity potentials inside the slip streams:

$$h = a_0 + \sum_1^\infty a_n \left(\frac{Z_1}{R}\right)^n \tag{49}$$

$$h' = a_0' + \sum_1^\infty a_n \left(\frac{Z_2}{R}\right)^n \tag{50}$$

By applying the matching conditions at the slip stream boundary, we obtain the following system of linear algebraic equations:

$$Re(h) = Re(H) \tag{51}$$

$$Re[R(\partial H/\partial r_1)] = Re[pR(\partial h/\partial r_1)] \tag{52}$$

$$Re(h') = Re(H') \tag{53}$$

$$Re[R(\partial H'/\partial r_2)] = Re[pR(\partial h'/\partial r_2)] \tag{54}$$

Thus, the constants are uniquely specified. The details of the calculations will not be given here as the resulting expressions are quite cumbersome. The total lift is given by an expression similar to Eq. (43), and Σ_s by an expression similar to Eq. (44).

The results of a numerical calculation for a wing with four propellers are shown in Fig. 9. The span loadings are quite conventional, except for a large increase in slope at the outboard slip-stream boundary. The cross-sectional areas Σ_s/A_s are presented in Fig. 6c (see Part I, previous issue).

References

[1] Munk, M., "Isoperimetrische Aufgaben aus der Theorie des Fluges," Inaug. Dissertation, Univ. of Gottingen, Gottingen, Germany (1919).

[2] Durand, W. F., *Aerodynamic Theory*, edited by W. F. Durand (Springer-Verlag, Berlin, 1935), Vol. II.

[3] Glauert, H., "The lift and drag of a wing spanning a free jet," British Aeronautical Research Council R&M 1603 (1934).

[4] Squire, H. B. and Chester, W., "Calculation of the effect of slipstream on lift and induced drag," British Aeronautical Research Council R&M 2368 (1945).

[5] Graham, E. W., Lagerstrom, P. A., Licher, R. M., and Beane, B. J., "A preliminary theoretical investigation of the effects of propeller slipstream on wing lift," Douglas Aircraft Co. Rept. SM-14991 (1953).

[6] Ribner, H. S. and Ellis, N. D., "Theory and computer study of a wing in a slipstream," AIAA Paper 66-466 (June 1966).